Are there optimum sites for global paleotemperature reconstruction?

Raymond S. Bradley
Department of Geosciences
University of Massachusetts
Amherst, MA 01003

Abstract

In order to place the relatively short instrumental record of global mean annual temperature in perspective, long proxy records are needed. Since it is unlikely there will ever be a globally extensive network of well-calibrated proxy records, it is necessary to identify sites which capture most of the variance of the larger scale average, to be used as representative time series for global means.

This problem is approached by examining different spatially extensive data sets (instrumental and GCM-derived) to determine the pattern of spatial correlation with the larger-scale mean series over different time-averages. A 1,000 year simulation (from the GFDL coupled atmosphere-ocean GCM) is used to examine the usefulness of various proxy indicator sites as predictors of global mean annual temperature series, for both inter-annual, and inter-decadal variations. Realistic networks of sites are used, representing locations where paleoclimatic records from corals, high latitude tree-rings, polar ice cores, mid and low latitude ice cores and mid-latitude historical and varved sediments have been obtained. From this limited set of sites, optimum networks are identified for both inter-annual and inter-decadal reconstructions. A combination of low latitude oceanic sites and interior continental locations seems to provide the best network for the reconstruction of global mean annual temperature.

Introduction

An understanding of the extent to which warming observed in the 20th century is due to human activity would be greatly enhanced if a reliable long-term record of global mean temperature was available. Such a record would shed light on the natural variability of climate prior to large-scale anthropogenic effects on the atmosphere. However, attempts to extend the intrumental record of global (or even hemispheric) mean temperature back beyond the early 19th century are inevitably doomed to failure due to the absence of widely distributed data sets prior to ~1850. For earlier periods, only high resolution paleoclimate records have the potential to provide annually resolved data as a proxy of climatic conditions in the recent past. Assuming the proxy records carry a strong, well-calibrated climatic signal (usually based on regression with parallel, instrumentally recorded data from the 20th century) a reconstruction of conditions prior to

NATO ASI Series, Vol. I 41
Climatic Variations and Forcing Mechanisms
of the Last 2000 Years
Edited by Philip D. Jones, Raymond S. Bradley,
and Jean Jouzel

the period of instrumental records can be made. What is often not clear is whether such an individual reconstruction represents only local conditions, or if it is representative of a wider region. If this was known, it might be possible to design an optimum paleoclimatic network which could be used to extend back in time the hemispheric or global mean temperature series (i.e. a network which contains most of the variance of such large-scale temperature series). To obtain the best paleotemperature reconstruction requires the judicious selection of an appropriate network of paleoclimatic proxy sites designed to optimise large-scale climatic signals. Identifying the appropriate sites (or more pragmatically, identifying only sites where proxy data are already available, or are being obtained) is the focus of this study.

It is worth noting that even if an optimum network of paleo data locations can be identified, several problems will remain:

a) proxy records rarely capture more than 50% of the variance of instrumental climate data series (i.e. are less than perfect recorders of climate);

b) most proxies are specific to one particular season.

c) proxy records may not capture variance equally well across all frequency bands; for example, some proxies may not be very helpful in representing low frequency changes due to problematical (non-climatic) low frequency characteristics of the proxy which have to be removed in signal processing (e.g. sediment compaction, tree growth effects). Such processing may eliminate (or change in some way) the true low frequency climatic signal in the data, yet it is precisely this signal which is of most importance in understanding the anthropogenic effects on global temperature.

Methodology

How representative is an individual site of larger scale conditions? This problem was examined by, *inter alia*, Briffa and Jones (1993) who computed the "correlation decay length" (l) for each node in a 5°(latitude) x 10°(longitude) grid of surface temperature data for the world (see also Madden et al., 1993, and the chapter by Jones and Briffa, in this volume). Maps of l were then presented which showed those areas where temperature variations were coherent over extensive areas (e.g. parts of the tropics and sub-tropics) as well as areas where there was far less coherence (e.g. northeastern North America and the North Atlantic Ocean). This study also showed spatial coherence is generally less in summer months than in winter. Briffa and Jones then went on to

select instrumental data from different regions and to regress that against the hemispheric mean temperature series; the regional data were then used to estimate the hemispheric time series, and to assess which region was most "representative" of the hemispheric mean series. Unfortunately, this approach can not be used to extend the hemispheric series back in time, as even regional temperature records are of limited duration. Only high resolution paleoclimate records (i.e. those having annual resolution) can be used to extend the hemispheric, or global, mean temperature series back in time over the last few centuries. The question is: what would be the ideal network of paleo data to use in reconstructing large-scale paleotemperature changes? To try to resolve this problem, I have turned to long-term simulations of climate variations produced by a coupled atmosphere-ocean general circulation model (AOGCM). The NOAA Geophysical Fluid Dynamics Laboratory's (GFDL) model (Manabe et al., 1991) comprises a 9 level, 4.5°(latitude) x 7.5°(longitude) atmospheric model, coupled to a 12 level 4.5°(latitude) x 3.7°(longitude) ocean model. The model uses a realistic geography, and seasonally varying insolation; it predicts cloud cover (as a function of relative humidity) and computes heat and water budgets over the continents (for further details of the model, see Manabe et al., 1990, 1991). The model reproduces well the modern distribution of temperature and the spatial characteristics of (inter-annual) temperature variance (when compared to instrumentally-recorded data). The model has been run for 1000 simulated years, without a change in external forcing, providing a unique set of globally distributed data which can be used to assess which regions of the world most closely capture the variance of hemispheric and global mean temperature *in this simulation*. The results may not apply to other model simulations or indeed to the real world, but nevertheless they provide a hypothesis which can then be tested in other data sets.

One problem with using the GFDL model results in this way is that there is a small downward trend in global temperature over the 1000 year simulation. This trend is due to problems resulting from the acceleration techniques used in the ocean phase of the model initialization (R. Stouffer, *pers. comm.*). Flux adjustments were made in the model, partly to control this drift, but the trend remains (Stouffer et al., 1994). Unfortunately, the overall global mean trend (-0.023°C per century) is not by any means the same at all grid points, being more strongly negative over much of the southern ocean and in part of the central North Atlantic (as much as -0.3°C/century at individual grid points), to positive trends (up to +0.07°C/century) in other regions (Figure 1). Thus,

depending on the location of the proxy site, it may be affected by these trends to a greater or lesser extent. Since the trends are largely model-dependent (the result of initialization procedures) and not related to forcing, the trend at each data point has been removed by simple linear regression. All subsequent analyses used this de-trended data set.

Annual data

Figure 2a shows a map of correlation coefficients between mean annual temperature at each grid point and global mean annual temperature, for the entire 1000 year run (similar patterns are also found for three 333 year sub-sets of the data). Figure 2b shows correlation coefficients for global mean annual temperature between individual grid points and global means for 1950-1979, based on instrumental data only. Although by no means identical, both analyses suggest that the inter-tropical zone is most highly correlated with global mean temperature, hence pointing to the need for proxy records from this zone if global mean temperature is to be accurately reproduced (cf. Briffa and Jones, 1993). Unfortunately, high resolution proxy records from tropical and equatorial regions are scarce (though likely to be less so in the future as new coral records are produced; see Dunbar and Cole, 1993 and chapters by Cole, Lough and Dunbar et al., in this volume). More common are proxies from mid and high latitudes, consisting of tree rings, varve sediments, historical records and ice core data. Realistically, we must accept a compromise between selection of optimum sites and sites where data are currently available, or are likely to be available in the near future. Accordingly, a number of "proxy networks" were identified (Table 1 and Figure 3). For each site, data from the nearest grid point in the GFDL model was selected and these were then correlated individually and in the form of network means, with the global mean temperature series, using only the last 200 years of data from the 1000 year model run (Table 2a). As expected, for global mean annual temperature, the coral networks were most highly correlated. By contrast, northern polar ice cap sites fared poorly. Indeed, the correlations generally decline latitudinally, from the coral and low latitude ice core networks, through the mid-latitude and northern treeline sites, to northern polar locations. Note that in this analysis no actual proxy data were used, only model-simulated data from each site; if actual proxy data were used, the correlations would probably be lower, depending on how well the individual record represents temperature variations.

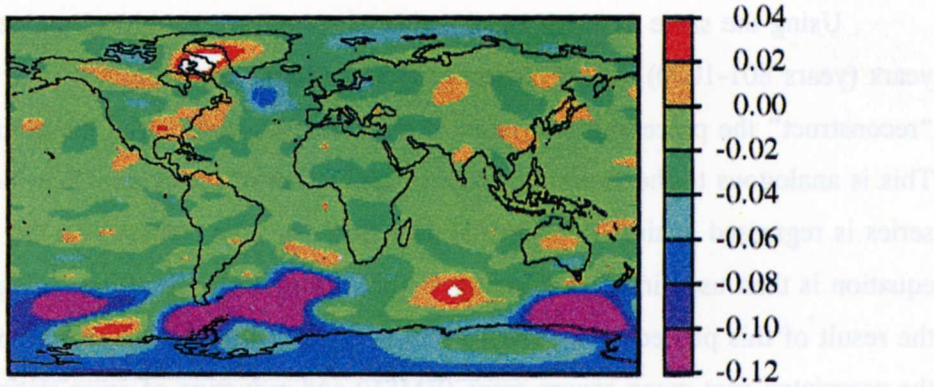

Figure 1. Linear trend of annual temperature in the 1000 year GFDL AOGCM simulation. Values range from extremes of -0.3°C/century to +0.07°C/century at individual grid points. The global mean trend is -0.02°C/century.

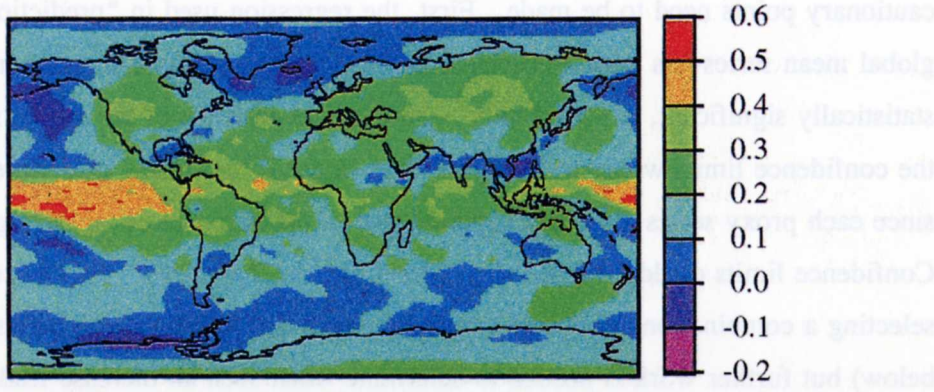

Figure 2a. Correlation coefficients between (de-trended) mean annual temperature at each grid point and the (de-trended) global mean annual temperature series, for a 1000 year simulation of climate using the GFDL AOGCM with no change in forcing.

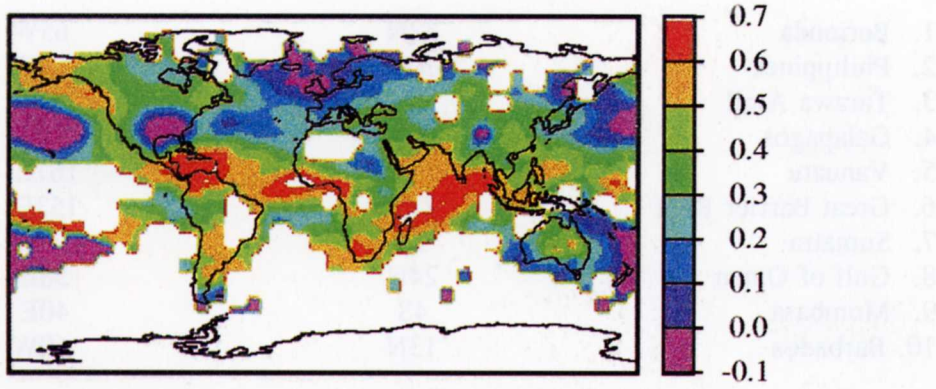

Figure 2b. Correlation coefficients between mean annual temperature at each grid point and the global mean annual temperature series, for instrumental data, 1950-1979. Extensive white areas represent regions with insufficient data.

Using the same network mean series regressed against global temperatures for 200 years (years 801-1000) the regression equations (Table 2b) were then used to "reconstruct" the preceding 800 years of temperatures variation in the global mean series. This is analogous to the approach taken in calibration of proxy data in which a proxy series is regressed against instrumental data from the 20th century and the resulting equation is then used in reconstructing the climate of earlier centuries. Figure 4 shows the result of this procedure for the 10 station coral network mean, and Table 2b shows the associated root mean square error (RMSE) and reduction of error statistic (RE) (Fritts 1976) for the years 1-800, comparing the reconstructed and actual series. Considering that only ten grid points are being used to estimate the variability averaged over 1960 points, the result is surprisingly good. Although these results are encouraging two cautionary points need to be made. First, the regression used in "prediction" of the global mean series has wide confidence limits (since the original correlation, though statistically significant, captured only $\sim 30\%$ of the variance of the global series); second, the confidence limits would probably be even larger if real proxy data were to be used, since each proxy series also only captures part of the variance of larger regional series. Confidence limits could be reduced by increasing the "predictor" network density, or by selecting a combination of different types of proxy data site locations (see section 6, below) but further work is needed to determine when such an increase leads to a point of diminishing returns.

Table 1: Locations of proxy data sites used in study.

A. Coral Sites	**Latitude**	**Longitude**
1. Bermuda	32N	65W
2. Philippines	10N	124E
3. Tarawa Atoll	1N	172E
4. Galapagos	0	91W
5. Vanuatu	15S	167E
6. Great Barrier Reef	22S	153E
7. Sumatra	2N	98E
8. Gulf of Oman	24N	58E
9. Mombasa	4S	40E
10. Barbados	13N	60W

B. Polar Ice Core Sites

11. Agassiz Ice Cap	80N	76W
12. Penny Ice Cap	67N	65W
13. Summit, Greenland	73N	38W
14. Dye-3, Greenland	65N	44W
15. Lomonosov Ice Cap, Svalbard	80N	25E
16. Franz Josef Land	81N	50E
17. Novaya Zemlya	76N	60E
18. Severnaya Zemlya	81N	95E
19. Mount Logan	60N	140W

C. Low Latitude Ice Core Sites

20. Quelccaya, Peru	14S	71W
21. Dunde, China	38N	96E
22. Guliya, China	35N	81E
23. Pamirs, Tadzhikistan	38N	74E
24. Tien Shan	42N	78E
25. Huascaran, Peru	9S	77W
26. Bolivia	16S	68W
27. W. Argentina	28S	69W
28. S. Chile	47S	73W

D. Mid-Latitude Historical Record, Tree-Ring or Varved Sediment Sites

29. Iceland	64N	22W
30. Switzerland	47N	8E
31. Smolensk, Russia	55N	33E
32. Nanjing, China	32N	119E
33. Tokyo, Japan	36N	140E
34. Sierra Nevadas, California	38N	120W
35. Charleston, S.Carolina, USA	32N	80W
36. Minneapolis, Minnesota, USA	45N	93W
37. Portland, Maine, USA	43N	70W
38. Novosibirsk, Russia	55N	83E

E. Northern Treeline Sites

39. N. Fennoscandia	68N	20E
40. N. Urals, Russia	67N	65E
41. Kamchatka, Russia	56N	161E
42. Upper Kolyma River, Russia	62N	150E
43. Arrigetch, Alaska, USA	67N	154W
44. Yukon, Canada	65N	138W
45. Barren Lands, Canada	64N	103W
46. Schefferville, Labrador, Canada	55N	67W
47. N. Siberia, Russia	72N	103E
48. Yakutsk, Russia	62N	130E

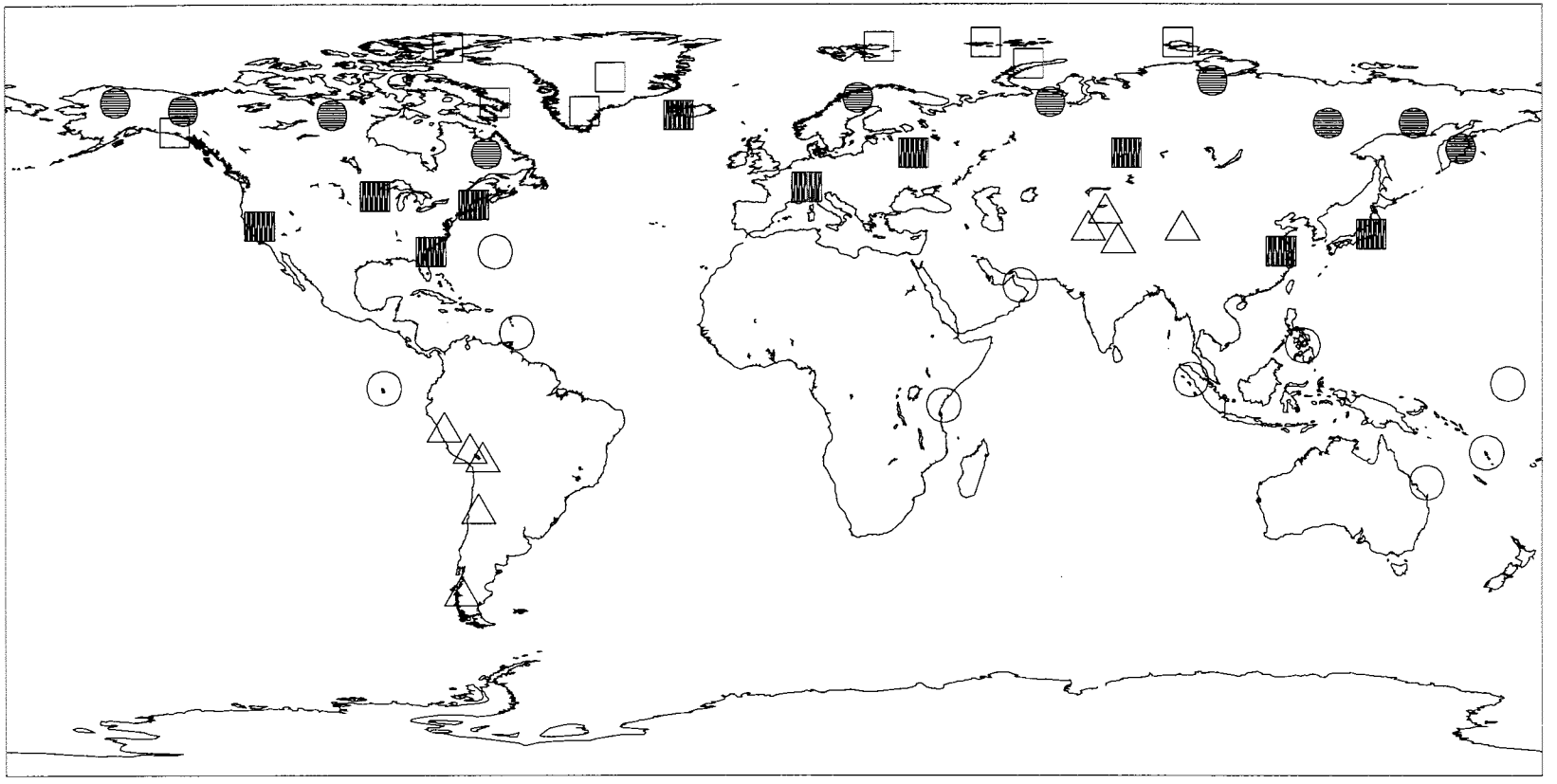

Figure 3: Distribution of the 48 proxy data sites used in this study. Open circles = coral sites; open squares = northern polar ice core sites; triangles = mid and low latitude ice core sites; closed circles = northern tree-line sites; filled squares = mid latitude tree-ring, historical records or varved lake sediment sites

Table 2a: **Correlation coefficients and significance level between network mean annual temperatures (averaged from sites listed in Table 1) and mean annual global temperatures, based on de-trended data for years 801-1000 in GFDL model simulations**

Network (cv Table 1)	r	probability
Corals	0.55	0.00
Low latitude ice caps	0.42	0.00
Mid-latitudes	0.38	0.00
Northern treeline	0.37	0.00
Polar ice caps	0.15	0.03

Table 2b: **Regression equation relating network mean temperature to global mean annual temperature, in years 801-1000 of the GFDL model simulation, and the correlation of model global mean annual temperatures in years 1-800 and global mean annual temperature "reconstructed" from network mean series using the regression equation. RE = reduction of error statistic; RMSE = root mean square error**

Network (cf Table 1)	Regression (years 801-1000)	r	RE	RMSE
		Years 1-800		
Corals	y = 0.361x + 0.002	0.55	0.32	0.079
Low latitude ice caps	y = 0.178x + 0.006	0.45	0.21	0.084
Mid-latitudes	y = 0.116x + 0.004	0.49	0.25	0.082
Northern treeline	y = 0.089x + 0.0008	0.38	0.15	0.088
Polar ice caps	y = 0.031x + 0.010	0.20	0.04	0.093

To what extent are these results an artefact of the GFDL model? Additional studies of other model simulations need to be carried out to answer this question, but here I examine the instrumental surface temperature data set to assess how well the same proxy series represent global mean annual temperature over the past ~100 years. Table 3 shows correlation coefficients between mean temperature series at grid points closest to the different proxy networks shown in Table 1. Both the coral network and the mid-latitude network capture 65% of the global mean temperature variance, but higher latitude series are much lower (sufficient instrumental data are not available for the polar network grid points). Figure 5 compares the global mean annual temperature record with that reconstructed only from grid points closest to the 10 coral data sites, though it should be noted that this comparison is for the "calibration" period (unlike Figure 4, which is for

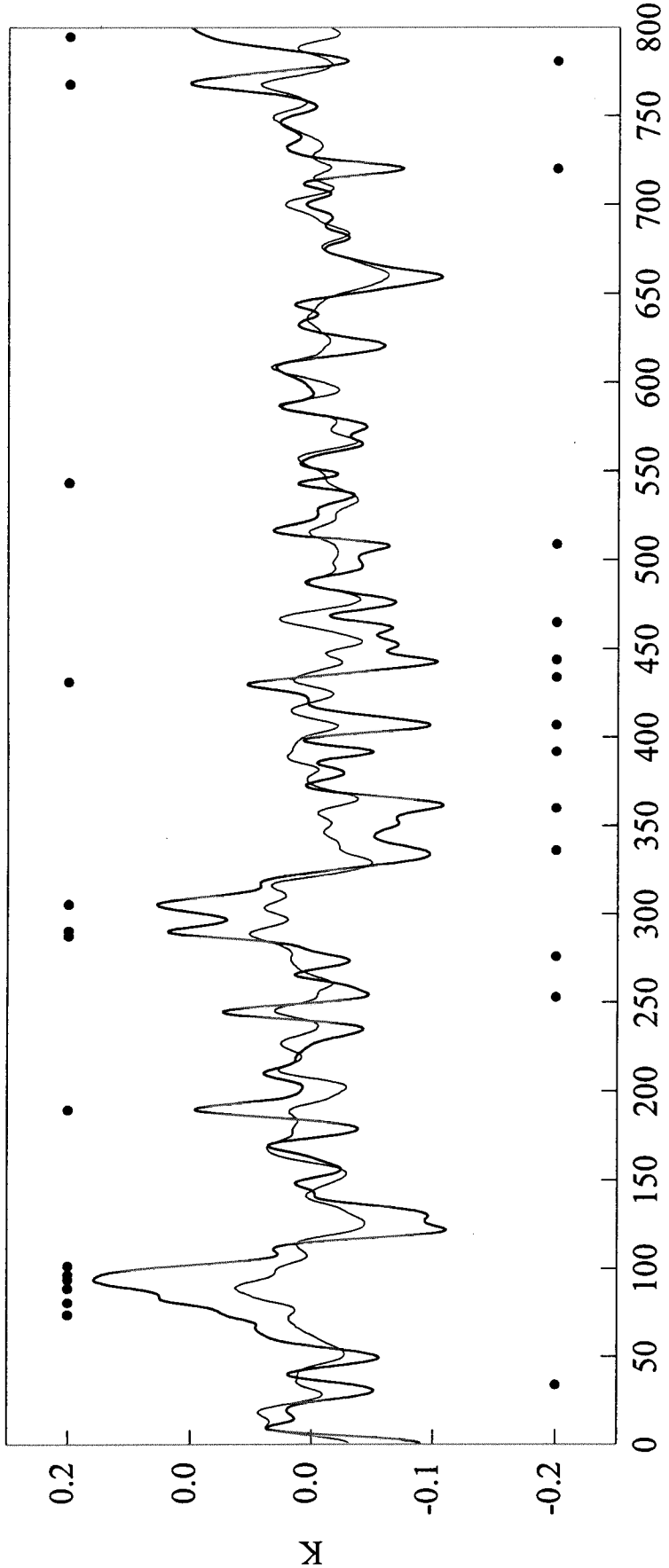

Figure 4: Reconstructed global mean annual temperature series in years 1-800, based on a network of coral sites (thin line), using a regression equation based on years 801-1000 only (cf. Table 2a and 2b). Original model global MAT series shown by thicker line. Both original data and reconstruction were smoothed with a 50 year gaussian filter. Values falling outside the 95% confidence intervals for the reconstruction are shown by black dots.

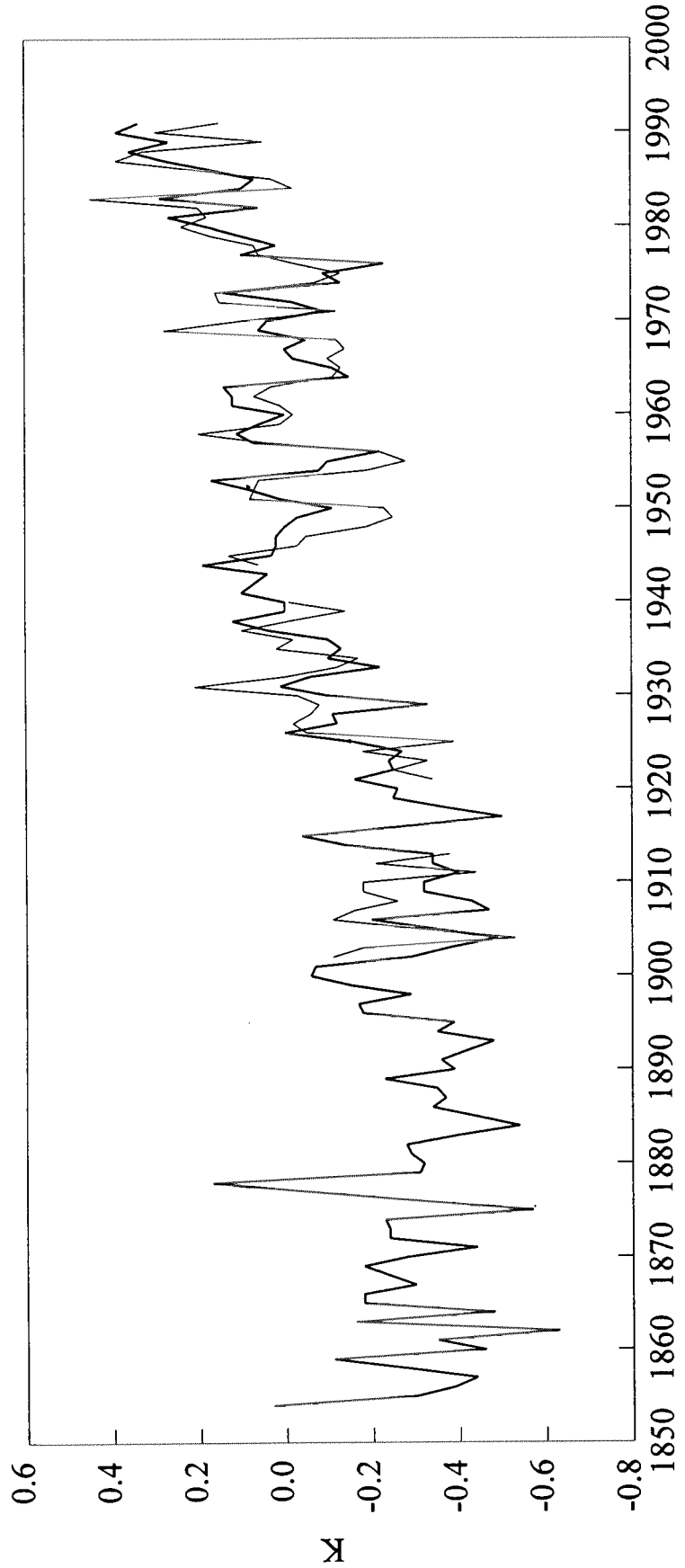

Figure 5 **Global MAT derived from spatially varying instrumental data (thicker line), compared to that reconstructed from a network of 10 grid points located nearest to coral sites listed in Table 1 (cf. Table 3).**

Table 3: Correlation coefficients between networks and global mean annual temperature for instrumental data (for all available years within the period 1851-1990

Network (cf Table 1)	r	probability	N
Corals	0.81	0.000	80
Low latitude ice caps	0.55	0.000	80
Mid-latitudes	0.81	0.000	132
Northern treeline	0.59	0.000	74
Polar ice caps*	-	-	-

* insufficient data for calculation

the "independent" period). I conclude that both the model and instrumental data analyses indicate the importance of low latitude proxy data sets to extend the record of global mean annual temperature back in time.

Decadal scale variability

In the previous section, I have focused on reconstructing inter-annual variations of temperature. For many purposes, this is less significant than being able to reproduce longer timescales of variability. To examine this question, all grid point data from the GFDL model were converted into decadal averages, producing a set of 100 values for each grid point. The procedures outlined above were then repeated. Table 4a shows the correlation coefficients between the network means and global MAT, for decades 81-100. Again, the coral series ranked highest, with overall correlations declining towards the higher latitude networks. Table 4b shows the corresponding regression equations and the correlations obtained between "reconstructed" global MAT and "observed". The coral network captured 50% of the variance of the global series and reproduces quite well its major features (Figure 6). By contrast, the polar network explains very little of the global mean temperature variance, either at the annual or decadal scale. I conclude that low latitude sites are important in representing both inter-annual and inter-decadal variability, based on the GFDL model results. This has been examined further by comparing the correlation field (spatial distribution of the correlation coefficient) between global MAT and individual grid points for data which has been filtered to remove variance below different thresholds (20 and 50 year periods). The spatial distribution of r for these filtered series (not shown) is very similar to that shown in Figure 2 (the un-

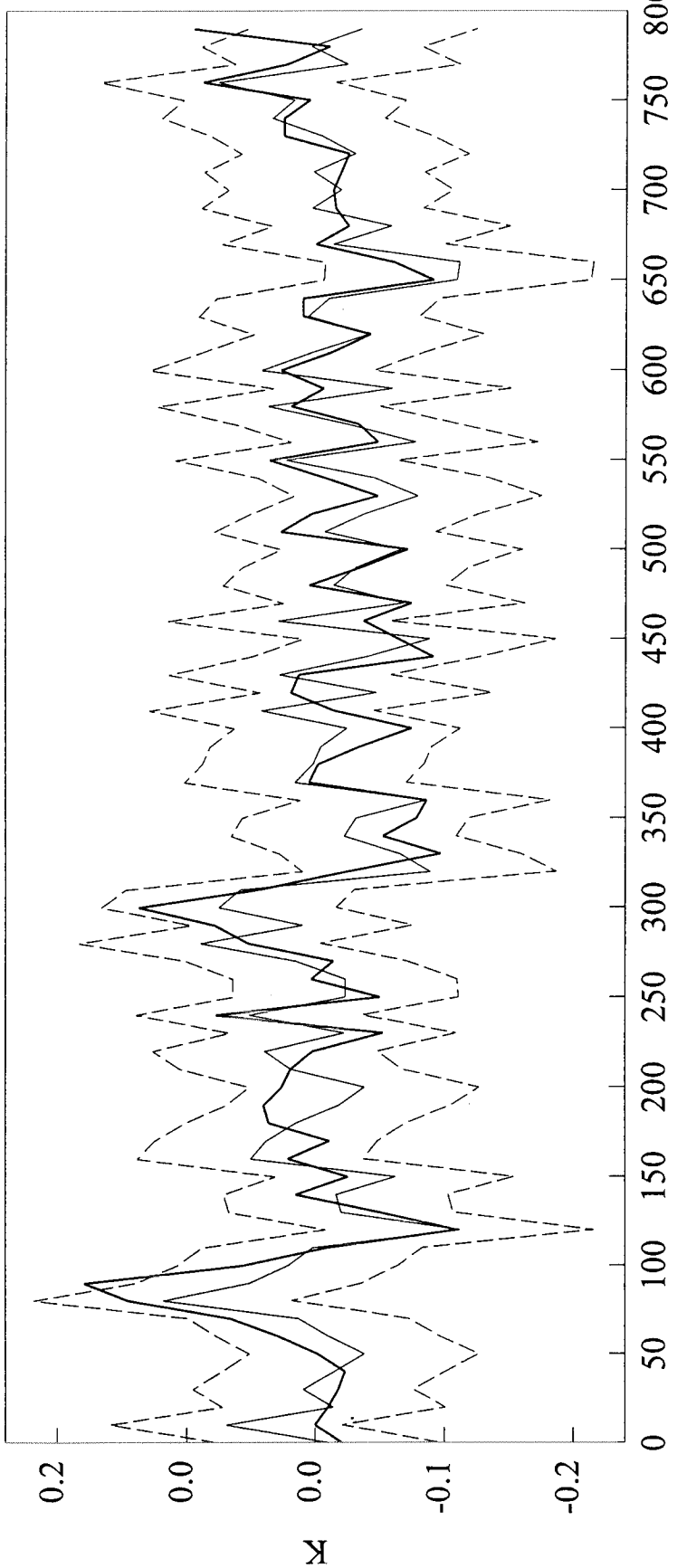

Figure 6: Reconstructed global *decadal* mean temperature series in decades 1-80, based on a network of coral sites (thin line), using a regression equation based on decades 81-100 only (cf Table 4a and 4b). Original model global decade mean temperature series shown by thicker line. 95% confidence intervals for the reconstruction are shown by dashed lines

Table 4: Correlation coefficients and significance level between network decadal mean temperatures (averaged from sited listed in Table 1) and decadal mean global temperatures based on de-trended data for decades 81-100 in the GFDL model simulations

Network (cf Table 1)	r	probability
Corals	0.71	0.000
Low latitude ice caps	0.69	0.001
Mid-latitudes	0.61	0.004
Northern treeline	0.49	0.028
Polar ice caps	0.07	0.078

Table 4b: Regression equation relating network mean temperature to global mean annual temperature in decades 81-100 of the GFDL model simulation, and the correlation of model global decadal mean temperature in decades 1-80 and global decadal mean temperature "reconstructed" from network mean series, using the regression equation. RE =reduction of error statistic; RMSE - root mean square error

Network (cf Table 1)	Regression (years 81-100)	r	RE	RMSE
		Decades 1-80		
Corals	y = 0.699x - 0.006	0.71	0.49	0.039
Low latitude ice caps	y = 0.416x + 0.000	0.69	0.51	0.039
Mid-latitudes	y = 0.305x - 0.007	0.59	0.28	0.047
Northern treeline	y = 0.170x + 0.006	0.43	0.22	0.049
Polar ice caps	y = 0.016x + 0.010	0.33	0.04	0.054

filtered, annual series) indicating that the networks discussed are important for paleotemperature reconstruction across a wide range of frequencies.

Optimum Networks

What is the optimum network for paleotemperature reconstruction? To answer this question, the correlations of individual grid points (from the 48 station network) with the global mean were first ranked. The 28 points with the highest individual correlations were then selected and used in an iterative analysis to identify the optimum 10 station network whose mean was most highly correlated with the global MAT series (the selection of a sub-set of 28 locations was arbitrary, in order to reduce the computational

time necessary; ideally, a network from all 1960 data points we be selected, but as this might identify sites where there are no proxy data, and no prospect of obtaining such data, the analysis was restricted to a very limited, but perhaps more pragmatic, sub-set of the overall network). Table 5 shows the overall "optimum 10 station network" which this analysis identified, and the associated statistics. This particular network only out-scored others by an insignificant margin, so it should be considered as one of several excellent networks which accounted for >50% of the variance of global MAT. Among the best performing networks, certain sites were often identified (Figure 7). These were: Tarawa Atoll (W. Pacific) Galapagos, Vanuatu, Barbados, Yakutsk (E. Russia) Sierra Nevada (California) Gulf of Oman, Quelccaya (Peru), Barren Lands (C. Canada) and Bermuda. Thus, some mix of equatorial/tropical oceanic sites (especially in the Pacific Ocean) plus sites in northern continental interiors seems to be required.

The analysis was repeated using only *decadal* average temperatures, as described earlier, and those stations most commonly selected are also shown in Figure 7. A number of networks were able to account for >80% of the variance of decadally averaged global MAT, and the optimum network accounted for >95% of the variance. Several sites commonly appear in both the annual and decadal "optimum" networks (Galapagos, Gulf of Oman, Bermuda, Peru [Huascaran/Quelccaya] and northeastern Siberia [Yakutsk]) again indicating the importance of low latitude oceanic and continental interior sites to obtain an optimum reconstruction of global MAT. Figures 8 and 9 show the reconstructions obtained from the annual and decadal optimum networks, compared to the first 800 years of the model global MAT series. It is clear that excellent reconstructions of the global mean series can be obtained with only a limited number of judiciously selected data points.

In a further attempt to identify critical sites, a stepwise multiple regression analysis was carried out, using decadal mean global temperature as the dependent variable, and decadal mean temperature at each of 24 individual grid points as independent variables, for the years 801-1000 in the model simulation. These 24 points were selected because they had the highest individual correlations with the global mean series. A multiple regression using data from four locations (Galapagos, Tien Shan [China], Sierra Nevada [California] and Huascarán [Peru]) was able to account for 90% of the variance of the global mean series (Figure 10). Galapagos alone explained 58% of the global decade-mean temperature record; the Tien Shan site accounted for a further 20%. These results

Table 5: "Optimum station networks"

1. *Annual Data* (10 best of 28 proxy sites with highest individual correlations)

Tarawa Atoll	S. Peru/Bolivia
Galapagos	Sierras, California
Vanuatu	Barren Lands, Canada
Gulf of Oman	N. Siberia (Khatanga River)
Barbados	Yakutsk, Siberia

Calibration: Years 801-1000

r	prob.
0.72	0.000

Reconstruction:

Regression (years 801-1000)	r	RE	RMSE
	(----------Years 1-800----------)		
y = 0.389x - 0.004	0.63	0.38	0.075

2. *Decadal Data* (10 best of 28 with highest individual correlations)

Galapagos	Switzerland
Gulf of Oman	Smolensk, W. Russia
Huascarán, Peru*	Minneapolis
Bolivia*	N. Siberia (Khatanga River)
S. Chile	Yakutsk, Siberia

Calibration: Decades 81-100

r	prob.
0.98	0.000

Reconstruction:

Regression (years 801-1000)	r	RE	RMSE
	(----------Years 1-800----------)		
y = 0.595x - 0.009	0.78	0.42	0.042

* Sites are closest to the same model grid point

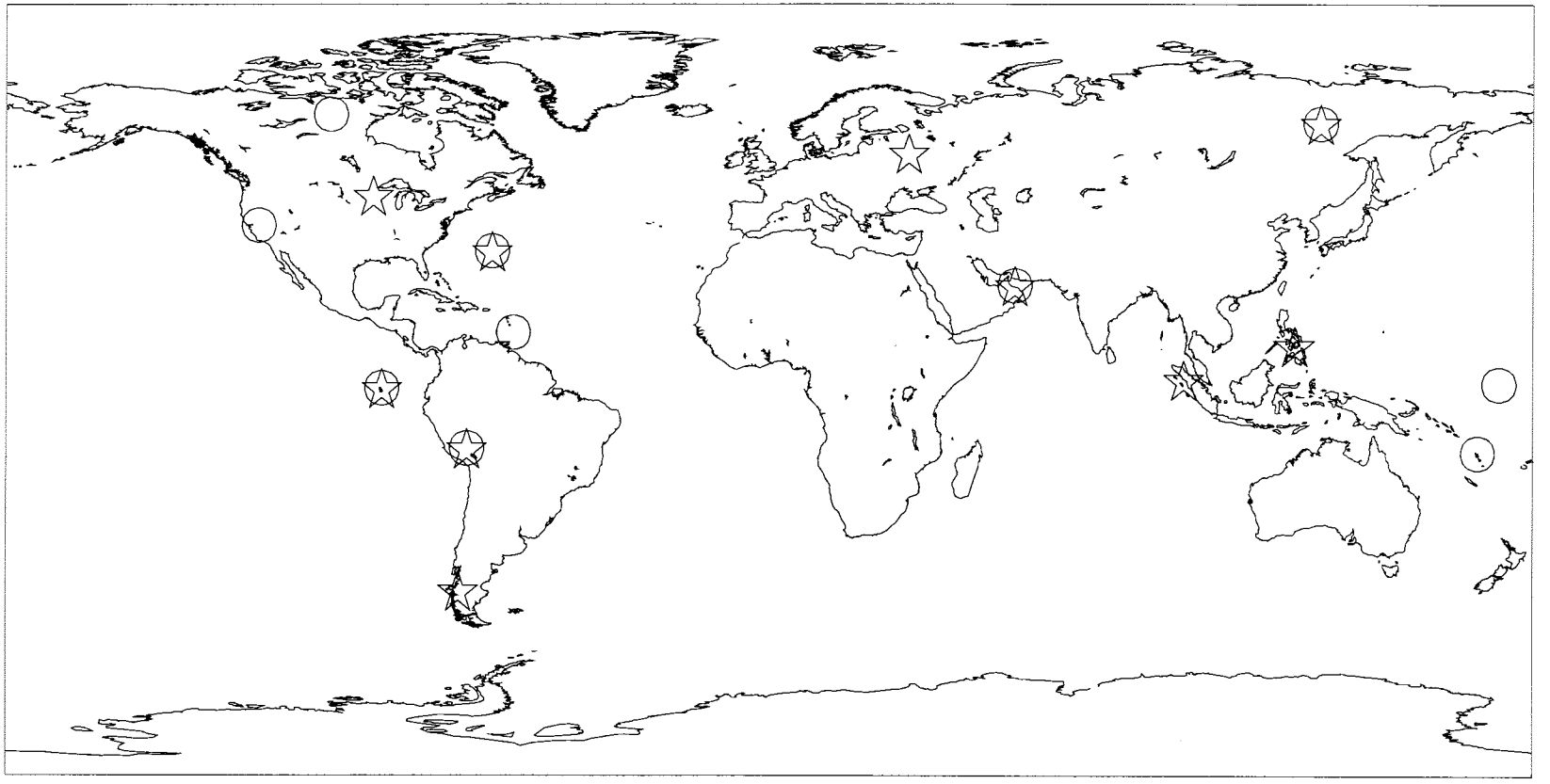

Figure 7: Locations which are identified in an "optimum site analysis" (see text) for annual data (circles) and decadal data (stars)

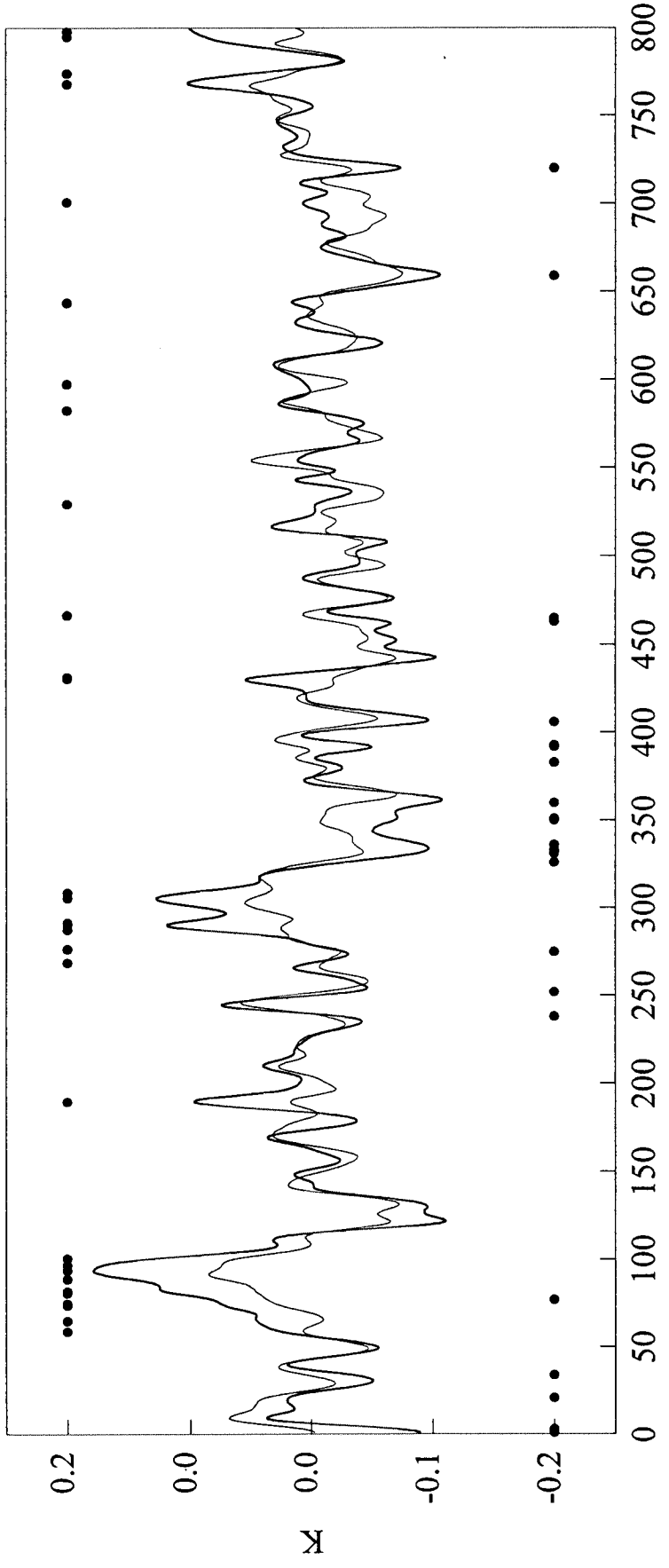

Figure 8: Reconstructed global mean annual temperature series in years 1-800 based on an "optimum" network of sites (thin line), using a regression equation based on years 801-1000 only (cf Table 5a). Original model global MAT series shown by thicker line. Both original and model data smoothed with a 20 year gaussian filter. Values falling outside the 95% confidence intervals for the reconstruction are shown by black dots

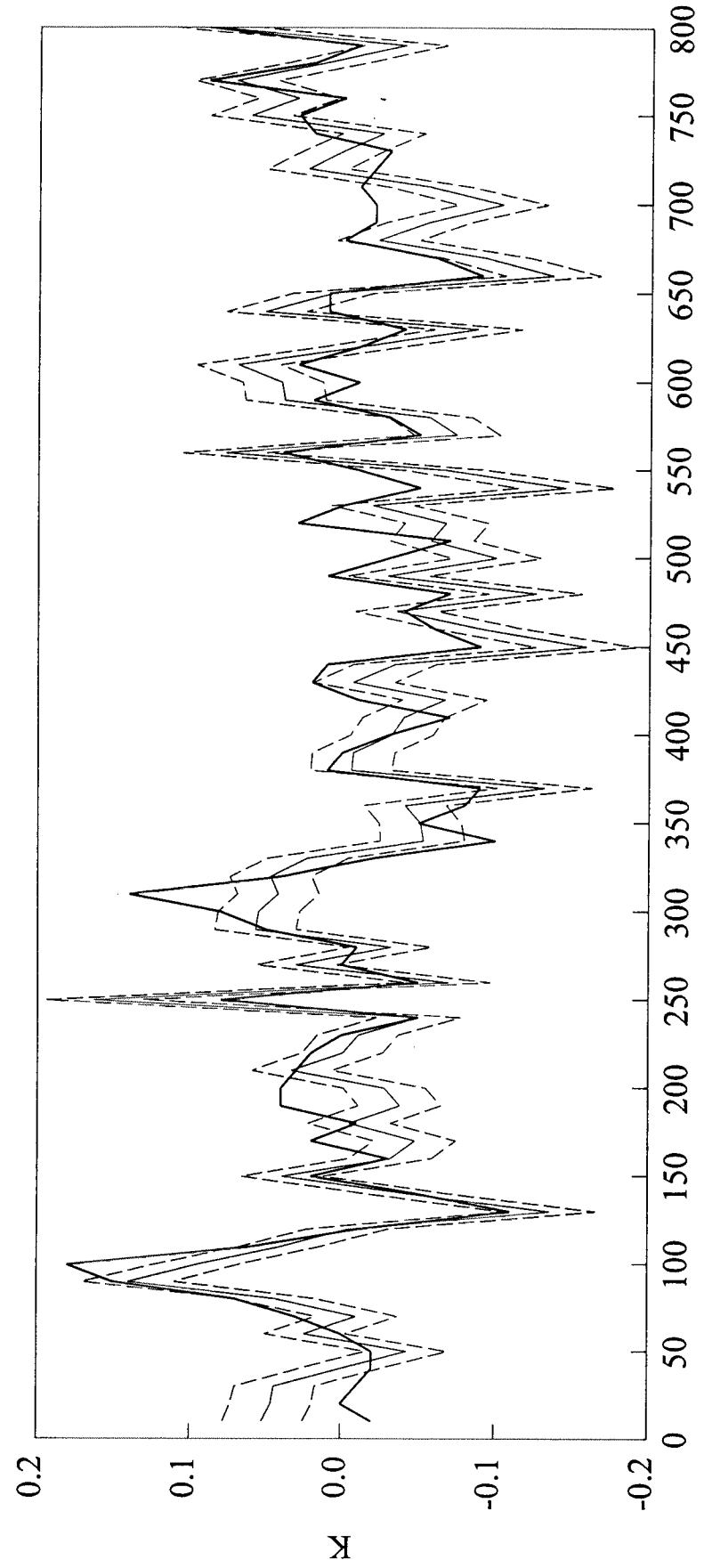

Figure 9: Reconstructed global *decadal* mean temperature series in decades 1-80 based on an "optimum" network of sites (thin line), using a regression equation based on decades 81-100 only (cf Table 5b). Original model global decade mean temperature series shown by thicker line. 95% confidence intervals for the reconstruction are shown by dashed lines

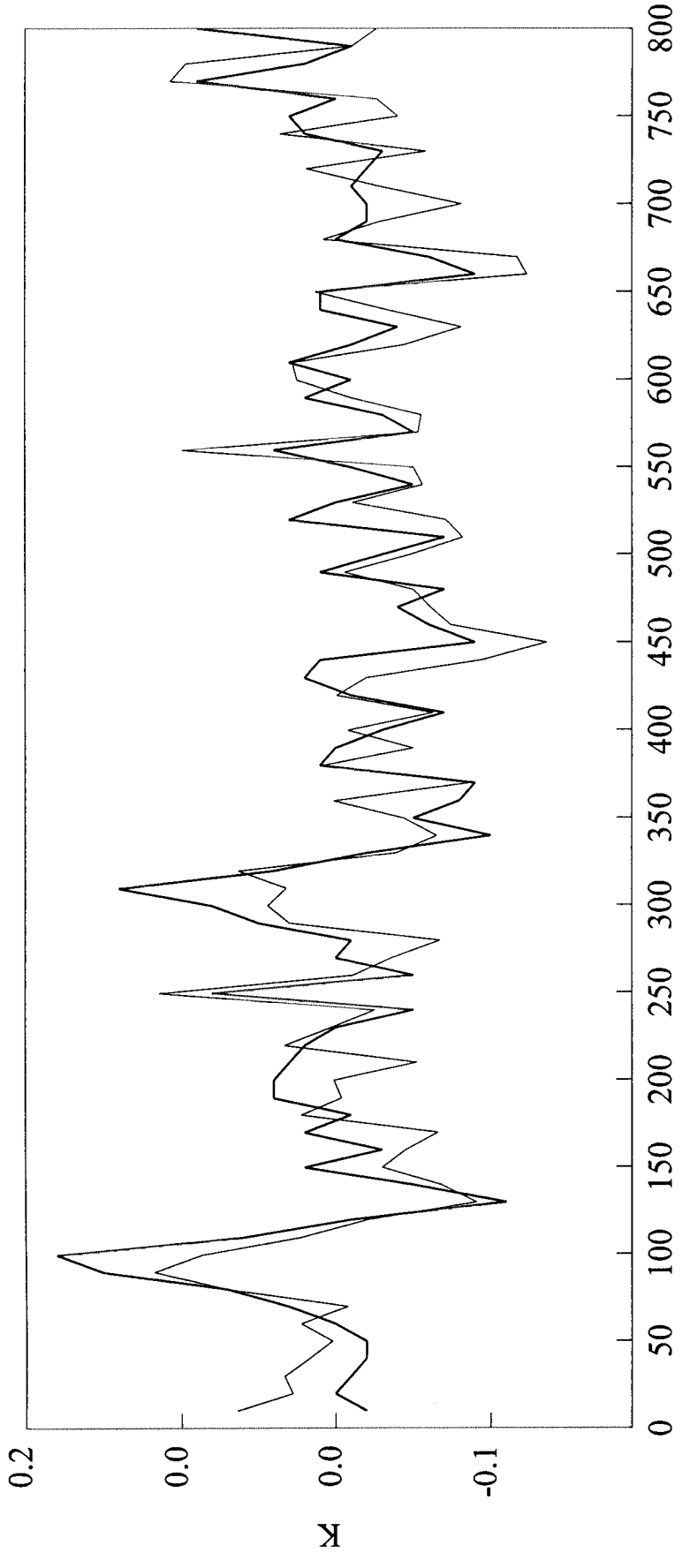

Figure 10: **Reconstructed global decadal mean temperature series in decades 1-80 based on a stepwise multiple regression equation derived from data in decaded 81-100 only. Four independent variables were selected from 24 locations (which, individually, were highly correlated with the global mean); the sites were: Galapagos (G), Tien Shan (T), Huascarán (H) and Sierra Nevadas (S) (cf Table 1). For decades 81-100, Y = 0.283G + 0.085T + 0.123H + 0.072S - 0.01; (R = 0.95). In the period of decades 1-80, the correlation coefficient (r) between the estimated (thin line) and model global mean data (thick line) is 0.70; RE = 0.362 and the RMSE = 0.044**

again suggest that a few sites can provide much information about large scale mean temperature variations, especially on decadal timescales (cf. Bradley and Jones, 1993 and chapters by Diaz, and Jones and Briffa, this volume).

Conclusions

A long simulation of surface temperatures from the GFDL AOGCM has provided insight as to where it would be most desirable to obtain paleotemperature data (starting with a limited set of options) in order to reconstruct global mean annual temperature back in time, and provide some perspective on global temperature variability before large-scale anthropogenic effects. A more comprehensive network would obviously be needed to reconstruct spatial patterns of past temperature. Obtaining proxy data from different sites may also be important in reconstructing other parameters. This analysis should, therefore, not be interpreted as minimising the significance of any particular data set. Furthermore, the results only reflect the statistical characteristics of the GFDL model simulation; much more research needs to be carried out to determine if these results can be generalised to other simulations, and indeed to the real world. Nevertheless, the results do point to the importance of low latitude oceanic sites in global temperature reconstruction. This conclusion applies to both inter-annual and inter-decadal timescales. Much of the variance of global temperature (especially on decadal time-scales) can be accounted for by selecting data from only a few sites. In an optimum network, a combination of both interior continental, and low latitude oceanic sites seems to be required.

Acknowledgements

I thank Drs R.J. Stouffer and S. Manabe for making available the results of their AO-GCM simulation, which form the basis of this paper. I also thank A. Robock and P.D. Jones for comments, and F. Keimig for computational assistance.

References

Bradley RS, Jones PD. (1993) "Little Ice Age" summer temperature variations: their nature and relevance to global warming trends. The Holocene, 3: 367-376

Briffa K, Jones PD. (1993) Global surface temperature variations during the twentieth century: Part 2: implications for large-scale high frequency paleoclimatic studies. The Holocene, 3: 77-88

Dunbar R, Cole J. (1993) Coral Records of Ocean-Atmosphere Variability. NOAA Climate and Global Change Program, Special Report No. 10, Washington D.C., 37pp

Fritts HC. (1976) Tree Rings and Climate. Academic Press, New York, 567pp

Madden RA, Shea DJ, Branstator DW, Tribbia JJ, Weber RO. (1993) The effects of imperfect spatial and temporal sampling on estimates of the global mean temperature: experiments with model data. J. Climate, 6: 1057-1066

Manabe S, Bryan K, Spelman MJ. (1990) Transient response of a global ocean-atmosphere model to a doubling of atmospheric carbon dioxide. J. Phys. Oceanog. 20: 722-749

Manabe S, Stouffer RJ, Spelman MJ, Bryan K. (1991) Transient responses of a coupled ocean-atmosphere model to gradual changes of atmospheric CO_2. Part 1. Annual mean response. J. Climate, 4: 785-818

Stouffer RJ, Manabe S, Vinnikov K Ya (1994) Model assessment of natural variability in recent global warming. Nature, 367: 634-636